Design and Verification of ALMA Band 9 Receiver Optics

A. Baryshev[1], R. Hesper[1], K. Wielinga[2], G. Gerlofsma[1], M. Carter[3]

[1]SRON, Landleven 12, P.O.Box 800, 9700 AV, The Netherlands.

[2]Mecon Engineering BV, Koopmanslaan 25, Postbus 679, 7000 BK Doetinchem, The Netherlands.

[3]IRAM, 300 Rue de la Piscine, Domaine de Universitaire de Grenoble, 38406, St. Martin d'Heres, France.

ABSTRACT

The Atacama Large Millimeter Array (ALMA) is an interferometer consisting of 64 antennae of 12 m diameter. It will be placed in Chile at a high altitude plateau (5000 m) with exceptionally good atmospheric conditions for astronomical observations at sub-mm wavelengths. The ALMA frequency coverage (30 GHz – 950 GHz) is divided into ten bands corresponding to the atmospheric transparency windows. The receiver for each band is mounted as a separate module in the ALMA front-end cryostat, which provides 4K, 12K, and 90K temperature levels.

We would like to report on the design of the ALMA band 9 (602-720 GHz) receiver module. A detailed optics layout for coupling between the telescope secondary and the SIS mixer feed horns will be presented. The local oscillator insertion optics will be described allowing for mounting a local oscillator module inside the receiver module at the 90K level.

To verify our intended production technique (CNC machining without any need for adjustment), a two-mirror prototype, representative of the signal path, has been produced. The output beam of this prototype was measured in phase-and-amplitude sensitive set-up. A superlattice device, used as a subharmonically pumped mixer, was mounted instead of the SIS device into the mixer housing. This allowed the evaluation of the optics (including the influence of machining tolerances) to be performed at room temperature. The receiver beam was measured in the near field at several signal frequencies using a Gunn-multiplier chain to generate the probe signal. A homodyne detection technique was used to retrieve both phase and amplitude, achieving a 60 dB signal-to-noise ratio. The measured patterns are then compared with theoretical predictions. Far-field beam patterns are computed from the measured near-field data allowing to predict the illumination of the telescope secondary mirror. Finally, the data was also used to verify if our CNC production method is suitable for production of mirrors with high enough quality for sub-mm wavelengths

INTRODUCTION

1.1 ALMA instrument

The Atacama Large Millimeter Array (ALMA) is an interferometric array of 64 heterodyne receivers. It will be located at an altitude of 5000 meters in northern Chile. This array is being built in collaboration between North America and Europe with Japan in the process of joining the project.

Each antenna consists of a 12 m diameter parabolic main reflector, a 0.75 m diameter secondary mirror. The receiver frequency coverage is 30-950 GHz. It is subdivided into ten bands, corresponding to the regions of high atmospheric transparency. For the first scientific operations four frequency bands were chosen: 3 (85–116 GHz), 6 (211-275 GHz), 7 (275-375 GHz) and 9 (600-702 GHz). All of these receivers are dual polarization and have either sideband separation or double sideband SIS tunnel junction mixers. A wide Intermediate Frequency (IF) bandwidth of 8 GHz was chosen as a baseline requirement.

The chosen mixer technology requires cryogenic temperatures of liquid Helium level (4K) and high vacuum. Due to the high number of systems to be produced, special attention should be paid to product/quality assurance [1,2,3].

1.2 ALMA front-end design

An artist impression of the ALMA front-end cryostat is shown in fig. 1. Each front-end holds 10 receivers housed in so-called cartridges and provides four temperature levels: 4K, 12K, 90K and ambient temperature.

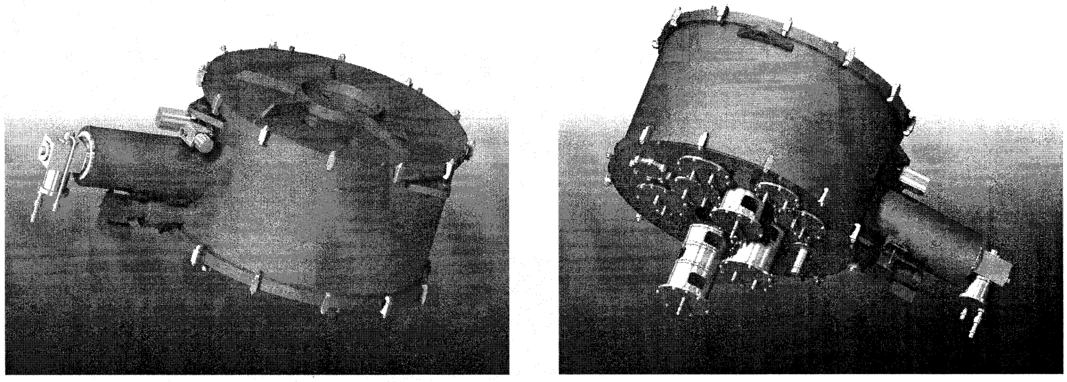

Fig. 1 Artist impression of the ALMA front-end cryostat holding 10 receiver cartridges. The design is done by the Rutherford Appleton Laboratory (UK).

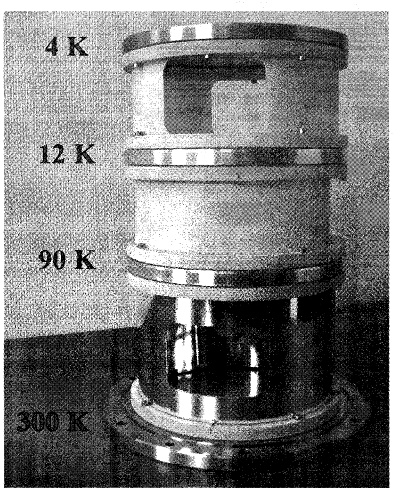

Fig. 2 Photograph of an ALMA cartridge structure.

The heat contact between the cryostat and the cartridge is provided by flexible links, allowing the insertion of the cartridges from the bottom of the front-end cryostat without accessing any internal structure [5]. The internal cryogenic connections are made automatically during cool down.

The telescope beam is entering the cryostat at the top, with the beam waist located near the cryostat window. Lower frequency bands have active optical elements (lenses and elliptical mirrors) mounted outside the cryostat vacuum space. However, for bands 5 – 10 all optics are contained within the cartridge at 4K.

The cartridge structure, on which all receiver elements will be mounted, is presented in fig. 2. A Sumimoto cryocooler provides four temperature levels (4K, 12K, 90K and ambient). The mechanical reference for the 4 K plate is provided through the cartridge support structure from the bottom of the cryostat. A finite element analysis was performed by RAL to ensure that the cartridge structure is rigid enough to perform within tolerance for all telescope elevation angles (from 0° to 90°).

BAND 9 OPTICS DESIGN

2.1 Design requirements and concept

The band 9 receiver optics has the following main design goals: a) all optics is mounted in the cartridge structure shown in fig. 2; b) the LO power source is located on the 90 K stage of the cartridge; c) most of the optics is located at the 4 K level; d) two orthogonal linear polarizations should be received from the sky; e) the secondary mirror illumination edge taper should be -12 dB and should not depend on frequency within the observing band; f) the design should be based on reflective optical elements; g) five waists beam clearance should be observed; and h) the cross polarization signal level should be less than –20 dB.

The ALMA antenna is a classical Cassegrain system, with an f-ratio of 8 for the beam entering the receiver. The receiver position is 0.1 m offset from main symmetry axis of the antenna.

Additional attention should be paid to the series production of the optics. The ALMA project requires 64 receivers to be built. Because of this requirement it was decided to build all the optics using conventional CNC machining and make machining tolerances sufficiently tight to avoid additional alignment procedure.

The frequency of band 9 requires a 7 micron RMS mirror roughness, and tolerances for the mirror surfaces of the order of 40 microns. These parameters are well within reach of up-to-date CNC machining techniques. Note that 7 micron RMS will not allow optical verification of the mirror alignment, and therefore use of a sub-mm wave antenna beam pattern measurement system is essential to asses the quality of the optical system. In order to verify the design concept and the applicability of direct CNC machining for these frequencies, a simple model of the signal

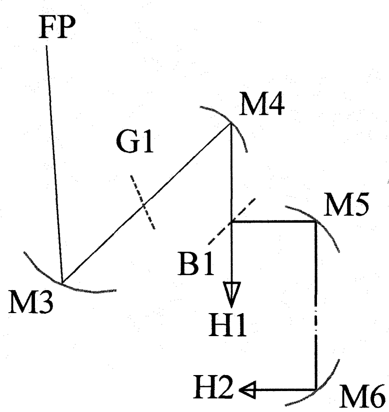

Fig. 3 Layout of optics. Beam dumps and one of the signal polarizations are not shown.

chain – a two-mirror block - has been built, together with a mixer horn, the details of it will be presented later in the section about measurement results.

2.2 Signal path

Drawing of signal path is presented in fig. 3. Telescope focus is located in the point FP. Two elliptical mirrors (M3, M4) are used to reimage the secondary mirror of telescope (M2) into the mouth of a mixer horn with the size, which is appropriate for -12 dB edge taper. The quarterly focal point (the second focal point of mirror M4) coincides with an apex of the corrugated horn H1. This construction allows for frequency independent coupling of the telescope beam to a corrugated horn feed. Mirror diameters are chosen to put through a 5 w size beam.

The second polarization beam is split off from the main beam at 90 degrees angle by means of a grid G1. The grid is located between mirrors M3 and M4 at the narrowest point of the beam (near tertiary focus). M3 is used for both polarizations and an additional mirrors M4', M5', and M6' are used for forming an orthogonal polarization beam arriving at second mixer horn H2. The cross polarization signals are absorbed by a special absorber plate mounted behind the grid G1 at 4K level.

2.3 LO insertion

Local oscillator signal is inserted quasioptically using a beamsplitter B1 in fig. 3. It is mounted between signal horn and mirror M4. A 12 micron Mylar film is used as beamsplitter material that corresponds to approximately 7% of LO signal insertion. The LO signal is then reflected towards 90 K plate of the cartridge where additional mirror M6 and final local oscillator multiplier (quintupler) is located. The quintupler beam is formed by a horn H2. The system is designed to put through a four waists size beam. Additional infrared heat filters are mounted on 12 K stage to decouple 4K and 90 K levels thermally.

The second polarization has its LO inserted in exactly the same way using mirrors M5' and M6' that are identical to M5 and M6 respectively. It has its own multiplier and horn H2'. This polarization is not shown in fig. 3.

An absorber plate is mounted behind each of the beamsplitters for both polarizations to dump LO power that is not coupled into the beam.

2.4 Opto-mechanical design

The layout that is briefly described below has to be realized in practice, i.e. mirrors, beamsplitters, grids and mixer horns have to be mounted within a certain tolerances with respect to each other and optics should be aligned. A tolerance budget was made for current optics layout indicating that 40 micron displacement is the highest requirement for displacement to produce 1% of efficiency loss [3,4].

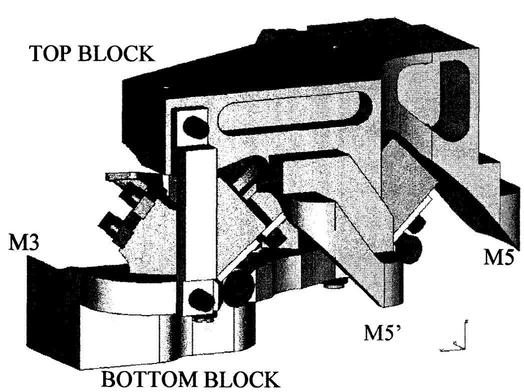

Fig. 4. Main signal optics design concept.

The main idea of the design is to make all the parts using CNC machining techniques observing tolerances. In this way all optics will be aligned upon assembly. Additional effort, like shimming or alignment using a lazer beam is not required. This allows for significant ease of requirements on mirror accuracy, grid foil flatness and beamsplitter foil flatness.

As it can be seen from the layout, mirrors M4, M5 and M4', M5' are pointing downwards. It is the most natural to make them out of one block during one CNC machining run. All beamsplitters and grids can be mounted in the block, also containing a mirror M3, which is directly machined in it. This concept is presented in fig. 4. The two blocks, bottom and top are

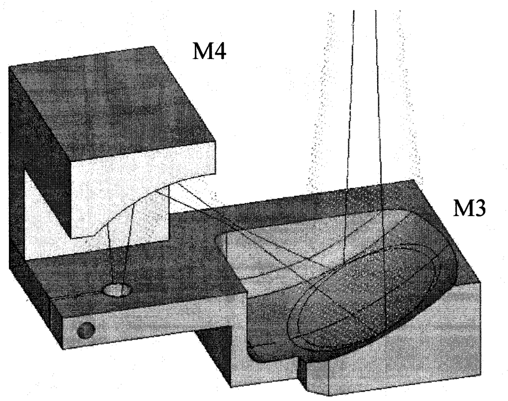

Fig. 5 A prototype two-mirror block for evaluating production techniques.

bolted to each other and interface is designed to keep these blocks within required tolerances.

2.5 Prototype mirror block

In order to verify if a selected machining techniques or design approach works a simplified model of a signal path consisting of two mirrors M3, M4 and mixer horn mount has been built as shown in fig. 5

MEASUREMENT SYSTEM

3.1 Scanning system and detection technique

A Measurement System: The measurements were made in the near field of the optics under test and similar to that described in [6]. A scheme of this system is shown in fig. 6. A small flared waveguide probe formed a transmitter beam in front of the receiver. Movements of the probe in the X, Y and Z planes were made in small discrete steps and at each point values of amplitude and phase were taken. The transmitter was a phase locked Gunn oscillator working between 100-120 GHz, which fed a X6 multiplication chain to have a transmitted signal between 600 and 720 GHz. A microwave synthesizer was used to drive a harmonic mixer within the phase lock loop. Signal of the same synthesizer was used as a LO for a detector. The intermediate frequency of 75 MHz was used the Gunn diode PLL circuit. An intermediate frequency of 75 MHz X 6 = 450 MHz can be detected by a subharmonically pumped mixer. A 450 MHz reference, coherent with IF signal, was created by multiplying the signal from 75 MHz PLL reference oscillator six times.

For most of the measurements a network analyzer with an access to internal reference and signal ports were used. This allows for using detection bandwidths up to 10 Hz (30 Hz was used in the measurements).

3.2 Standing waves compensation method

A standing wave in the setup was suppressed by using the following technique. Two data points were taken with lambda over four separation in z-axis. These two points were added up with correction of the phase of Pi over two. The forward signal is than added constructively, unlike the first order reflections, which has a phase difference of Pi. These reflections are added destructively. This method allows to effectively suppress parasitic effects due to first order reflections for beams, close to a parallel. Band 9 receiver f#8 beam is slow enough to achieve good standing wave suppression without degrading the quality of measurement itself. Additionally, an absorber plate around the

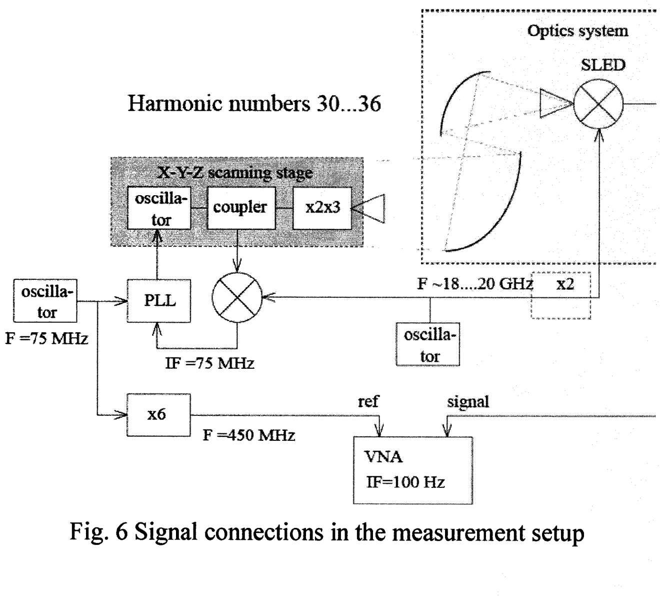

Fig. 6 Signal connections in the measurement setup

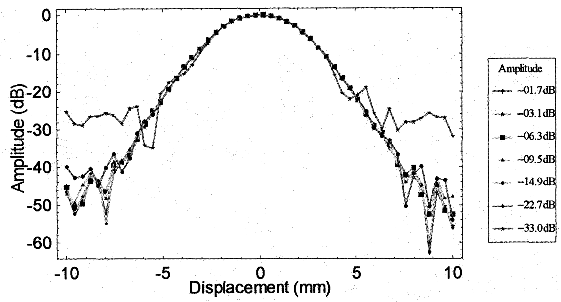

Fig. 7 Normalized amplitude field distribution measured at different signal source levels to check for a detector saturation effects.

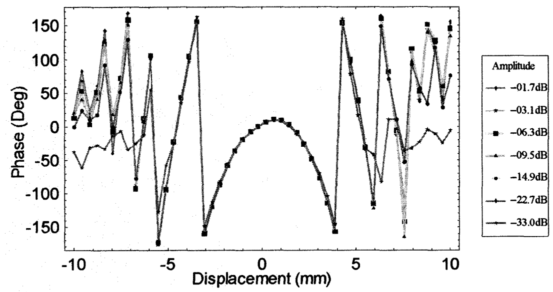

Fig. 8 Normalized phase field distribution measured at different signal source levels to check for detector saturation effects.

source was used to damp reflections.

3.3 Room Temperature detector and saturation

An SLED (super lattice electronic device) [7] was mounted instead of an SIS junction in one of our mixer holder to ensure that system under test fully represents mechanically the final receiver. This detector potentially has better conversion efficiency as conventional diode. Although, no specific matching circuit was designed to couple the SLED to an RF environment, signal to noise ratio of 72-80 dB has been obtained for all frequencies in ALMA band 9, using about 50-70 microwatt as an input signal. All measurements were done at room temperature. The SLED was pumped subharmonically. 36th harmonics of LO was typically used.

Since SLED is relatively new detector device for this type of measurements, special attention was paid for detector saturation by the input signal. To check this effect, subsequent measurements were done for a corrugated horn while only changing a source output power. Results of this measurement are presented in fig. 7 and 8 for amplitude and phase respectively. No significant compression was found in the data as well as phase appears to be stable even for very significant drop (-33 dB) of input signal power.

MEASUREMENT RESULTS

4.1 Laser beam propogation

The two-mirror block, presented in fig. 5 was produced by a CNC machining technique. Mirror surfaces were machined by a boll mill in the 5-axis CNC machine. After light polishing, the surface quality was good enough to put through a laser beam. The beam itself can be visualized by applying a water vapour fog during long time exposure of digital camera. The result is shown in fig. 9.

Intermediate (tertiary focus) and final (quarterly focus) are clearly visible. Some beam splitting can be observed at lower right corner of the picture. This is due to approximation errors that occur during milling of the mirror surface. Note that frequency, at which the effect is observed, is 1000 times higher than the required frequency.

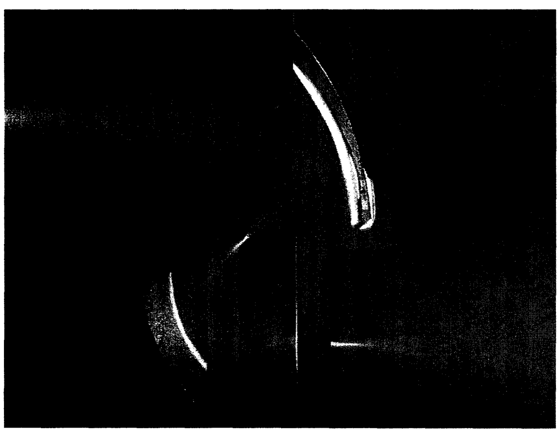

Fig. 9 Laser beam sent through machined two-mirror block.

4.2 RF beam pattern measurement and analysis

A 2-D plot of amplitude and phase beam distributions are shown in fig. 10 and 11 respectively. The mirror symmetrical axis coincide with Y-axis of scanner. One can see that a central maximum has a symmetrical shape both in phase and amplitude. A low levels of sidelobes are observed. A round ring structure at lower levels can be explained by periodical deviations of mirror shape from nominal curve due to machining strokes of the mill tool.

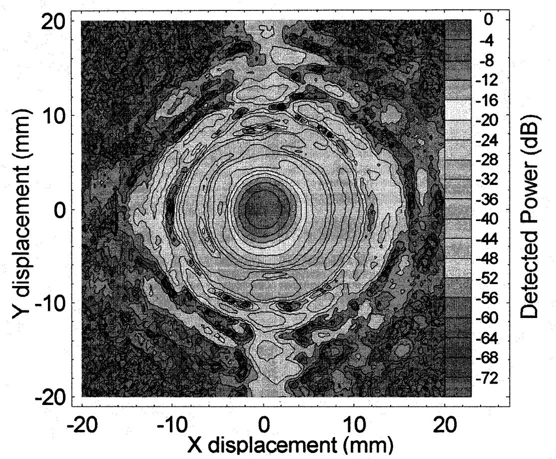

Fig. 10 Measured near field beam amplitude distribution of the two-mirror block at -50 mm from the waist plain. Frequency is 672 GHz.

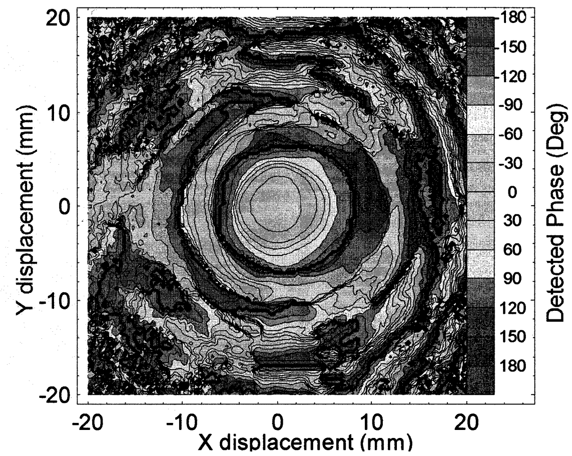

Fig. 11 Measured near field beam phase distribution of the two-mirror block at -50 mm from the waist plain. Frequency is 672 GHz.

Amplitude and phase information allows to calculate an overlap integral of the measured data with fundamental mode Gaussian beam. Ideally, this beam has six parameters, which can be determined from the data by maximizing Gaussian beam coupling. These parameters are: beam waist size, waist position (X,Y,Z), and two beam tilt angles. If the scanning plane is referenced to a mirror surface by a calibration device, obtained parameters allow to conclude about the production and mounting errors

frequencies. and the efficiency loss. The Gaussisian beam efficiency of the beam shown in fig. 10-11 is about 98%, which is very close to a theoretical predictions. The waist size, offsets and tilt angle are within the required

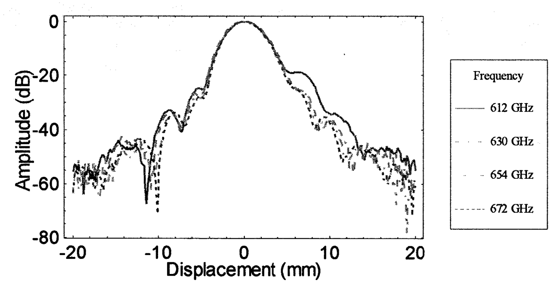

Fig. 12 Normalized amplitude field distribution measured along mirror asymmetrical axis at different signal frequencies.

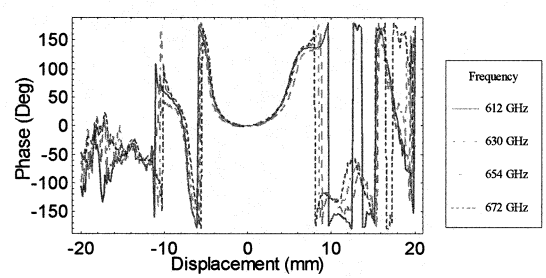

Fig. 13 Normalized phase field distribution measured along mirror asymmetrical axis at different signal frequencies.

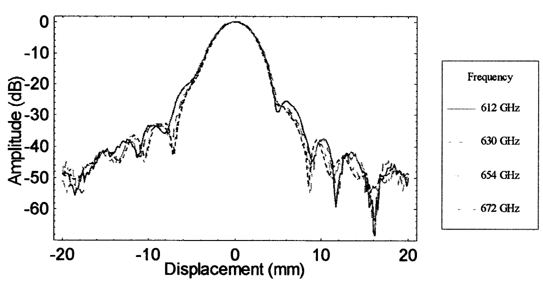

Fig. 14 Normalized amplitude field distribution measured along mirror symmetrical axis at different signal

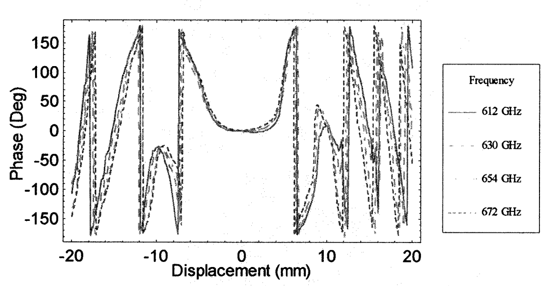

Fig. 15 Normalized phase field distribution measured along mirror asymmetrical axis at different signal frequencies.

tolerances. The efficiency loss is less than 1%.

Measured beam cross-sections both for symmetrical (Y) and asymmetrical (X) mirror axes are shown in fig. 12-15. These measurements were done for several frequencies in ALMA band 9. Note that beam quality maintains over whole frequency range except the lowest frequency. At the lowest frequency, some deviation can be explained by a corrugated horn beam pattern change. A new horn design is underway.

As expected, the beam is largely symmetrical for symmetrical mirror axes. Visible aberrations effects are present in the cuts along the asymmetrical mirror axes. These effects, give rise to a beam tilt with respect to a nominal beam direction. Beam tilt, determined from measurements, is still within the required boundaries.

Finally, a far field antenna beam pattern can be determined from the 2-D data of fig. 10-11 by means of 2D Fourier transform. The resulting amplitude angular distribution is shown in fig. 16 and central part of the distribution is shown in fig. 17 compared with the angular size of ALMA antenna secondary mirror. Since mirror is in the far field zone of the waist, this gives a good indication of the illumination edge taper. From fig. 17 one can conclude that the edge taper is very close to the required 12 dB and illumination pattern of the secondary is well centered. A semi-round fringes are visible at the beam pattern at very low signal levels. These fringes are again due to approximation error of the CNC machine (and due to tool stroke direction). However, still visible, these effects do not degrade significantly the illumination pattern at the secondary mirror.

Periodical mirror surface deviations produce a various peaks at far field pattern, see fig. 16. The angle of these peaks allows to determine the period of these deviations. Random deviations with white spectrum result in increase of a spill over from the main beam towards all directions uniformly. Good signal to noise level obtained in the figure and low level of peaks due to periodical deviations suggests that the selected production technique is sufficient for application in ALMA band 9 receiver.

CONCLUSION

An opto-mechanical layout of ALMA band 9 receiver is proposed. A production method of direct CNC machining of mirror surfaces and alignment of optics by assembly was demonstrated by building a prototype optics system and developing a near field beam pattern measurement system. The proposed technique proves

to be successful and can be applied for not only for ALMA band 9 but also for any ground based or space instrument requiring to build many copies of optics, for instance a free flying interferometer.

A super lattice electronic device (SLED) detector was successfully used as a replacement of an SIS junction for room temperature evaluation of optics layout. A signal to noise level as high as 80 dB has been achieved for 30 Hz

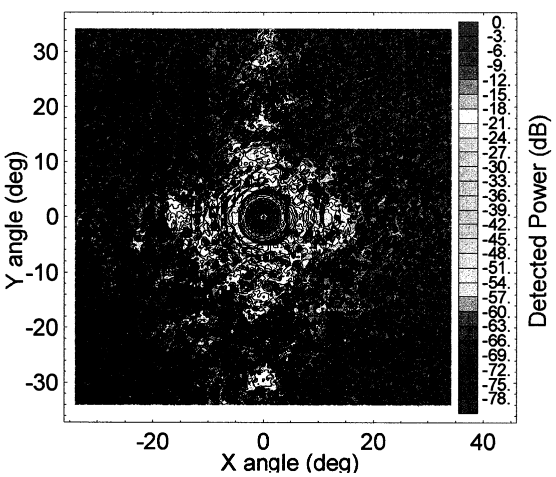

Fig. 16 Calculated far field amplitude angular distribution of the two-mirror block. Frequency is 672 GHz. The boundary of secondary mirror and central blockage of antenna are presented by a dashed line.

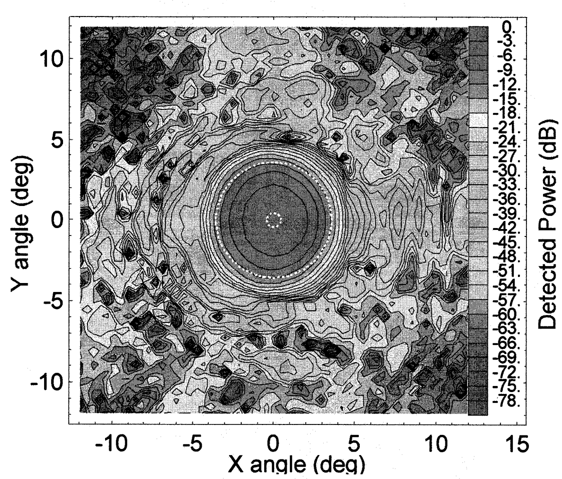

Fig. 17 Calculated far field amplitude angular distribution of the two-mirror block. Frequency is 672 GHz. The boundary of secondary mirror and central blockage of antenna are presented by a dashed line.

detection bandwidth at 672 GHz signal frequency for room temperature detector.

ACKNOWLEDGEMENT

The authors would like to thank Mark Harman of RAL for the overall design of the cartridges and cryostat that were given in section 1.2 We would also like to thank Fabrice Coq for the help in making the measurements. We would like to thank Willem Jellema for help in developing beam pattern measurement system. Authors also would like to thank Paveliev D.G. for providing SLED devices and Th. De Graauw for stimulating discussions. This work was supported by European Southern Observatory as a part ALMA band 9 contract.

REFERENCES

[1] ALMA Receiver Optics Design, J.Lamb et al, ALMA memo 362

[2] ALMA Project Book chapter 5, W.Wild et al.

[3] ALMA Front-end Optics, M.Carter et al, to be published

[4] ALMA Receiver Optics 2nd report, C-Y.Tham, S.Withington ALMA EDM

[5] ALMA project Book, chapter 6 Cryogenics, A.Orlowska et al

[6] Phase and Amplitude Measurements on an SIS Mixer fitted with a double slot Antenna for ALMA Band 9, M.Carter et al, Proceedings of The 13th International Symposium on Space Terahertz Technology

[7] Schomburg et al, Electronics Letters, vol 35, No 17 (1999)